CMUTs for Air Coupled Ultrasound with Improved Bandwidth

Mario Kupnik*, Min-Chieh Ho†, Srikant Vaithilingam†, and Butrus T. Khuri-Yakub†
*Brandenburg University of Technology (BTU), Cottbus, Germany.
† Stanford University, CA, USA.

***Abstract*—We present the design, fabrication and characterization of a multi-purpose capacitive micromachined ultrasonic transducer (CMUT) for air coupled ultrasound (∼300−500 kHz), with a focus on improved bandwidth. The focus of this work is to investigate whether and how wafer-bonded CMUTs can be improved in terms of bandwidth for airborne ultrasound by intentionally varying the cell radii across the entire device. Further, we consider the differences in terms of static d.c. operation point for improved frequency response and predictability by using a sensitivity-weighted distribution of cell radii groups. The pitch-catch results from one of our designs, compared to a reference device (all cell radii identical), show that the -6 db fractional bandwidth (FBW) can be improved from 1% up to 2.5%. For many applications, in which the -14 db duration signal (ASTM E1065) plays a role, the improvement goes from 1% to 18.9%. The observed improvements support the argument that such CMUTs will be beneficial for ultrasonic transit-time detection based applications.**

I. Introduction

In wafer-bonded CMUTs with plates made of single-crystal silicon from silicon-on-insulator (SOI) wafers and evacuated cavities, the bandwidth is low when operated in air. Typical quality factors range from Q ∼10 to 400, depending on the transducer geometry, biasing condition, and thickness uniformity of the SOI wafer used (polished or epitaxial grown).

In previously designed CMUTs for chemical sensing applications, an impressive quality factor of 400 was measured for 1000 CMUT cells, connected and operated in parallel [1].

Many other applications, however, require a low quality factor for airborne ultrasound applications. Examples are range-finding applications, ultrasonic transit-time gas flow meters for metering dynamic gas flows, anemometry applications, and various other ultrasound-based sensing applications.

The main idea of this work is to investigate whether and how wafer-bonded CMUTs with evacuated cavities can be improved for airborne applications by intentionally varying the cell radii across the entire device. Further, the distribution of cell radii in our devices is weighted by the displacement sensitivity of each cell radii group.

We do not consider a sparse CMUT cell placement in the transducer, as proposed in [2]. This is mainly because we intentionally limit the design freedom in terms of cell geometry and active area, which allows us to perform a direct comparison to a reference device, having the same number of cells (all with identical radius).

Further, this work is only focused on airborne ultrasound, and not on immersion, such as described in [3], [4].

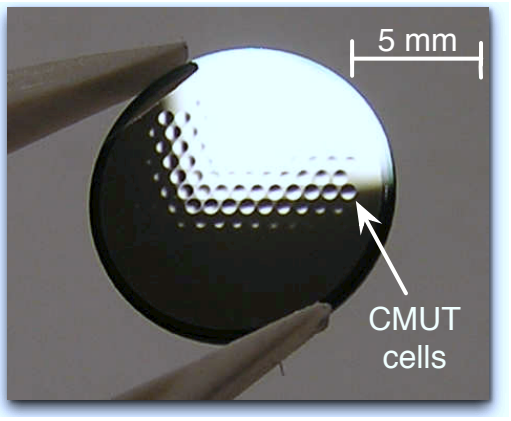

Fig. 1. Photograph of a multi-purpose CMUT for airborne ultrasound applications. Some of the 163 deflected CMUT plates (circular shape) are visible.

II. Design and Device Fabrication

We used a previously published fabrication process [5], which starts with an SOI wafer with a thick buried oxide layer ("thick-box process") as substrate. The process is simple and improves the reliability and performance of wafer-bonded CMUTs in terms of electrical breakdown and reduced parasitic capacitance, respectively. By etching vertical trenches down to this BOX layer, each CMUT cell has its own electrode,

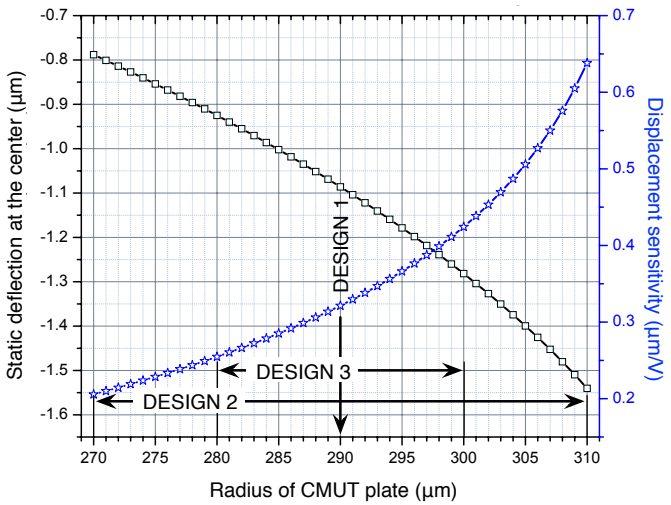

Fig. 2. Simulation results based on finite element analysis, used to decide on a displacement sensitivity-weighted cell radii distribution.

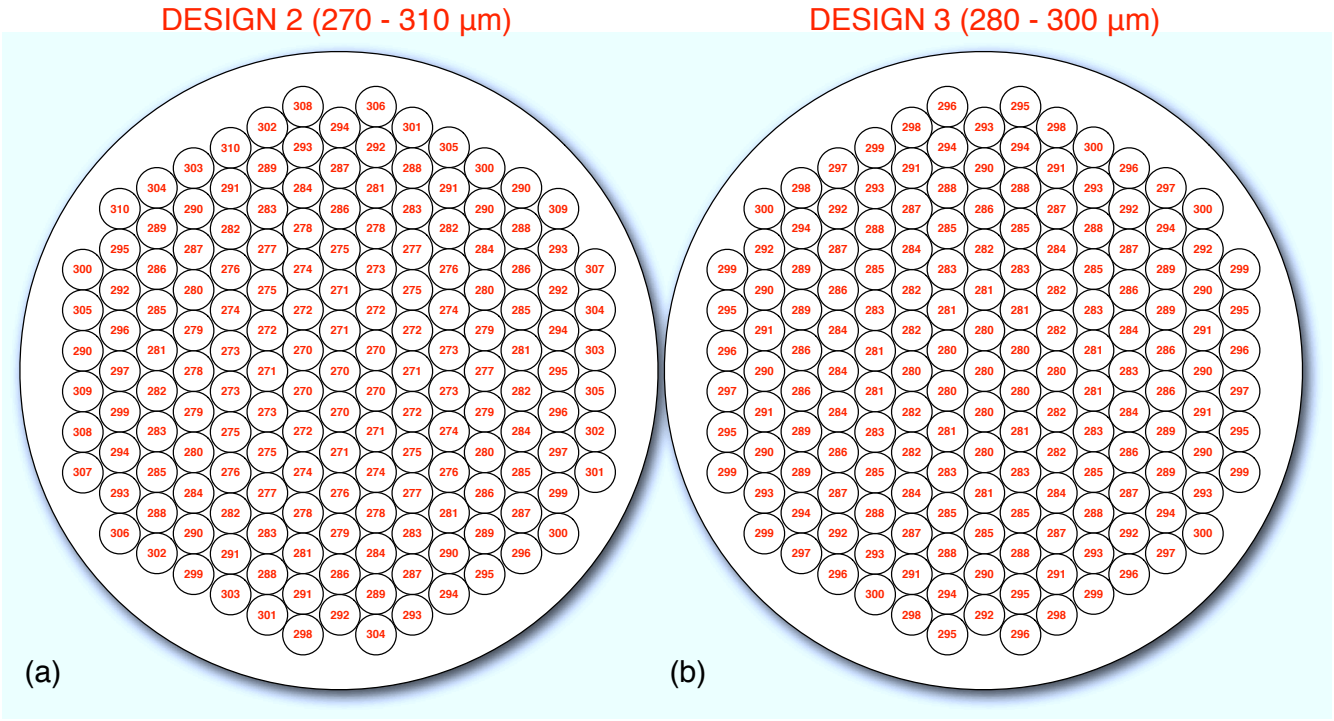

Fig. 3. Layout of radii distribution on the devices of DESIGN 2 (a) and DESIGN 3 (b). The center location of each cell is identical as in DESIGN 1.

connected through a via to the backside of the wafer. This ensures that the high-electric field is only where needed, i.e. in the vacuum gap below the moving plate, and, in addition, the insulation layer in the post area is not permanently stressed by the applied d.c. voltage. A detailed description of the advantages and fabrication steps can be found in [5]–[7].

Three different designs of devices have been fabricated: DESIGN 1, the reference device (Fig. 1 shows a photograph), and two variations of the new design (DESIGN 2 and 3, their layouts are shown in Fig. 3). The reference device (DESIGN 1) has only one cell radius of 290 μm, for DESIGN 2 and 3 the radii are varied. The main difference between DESIGN 2 and 3 is the range of values from which the radii are varied (Fig. 2), but for both new designs the step size of the radius variation is 1 μm. Thus, for DESIGN 2 we use 41 different cells and for DESIGN 3 we use 21 different cells.

All device have a total number of 163 CMUT cells, evenly distributed over the entire device. The diameter of the CMUT is 11.85 mm and the center locations of all the cells are identical for all three designs (see Fig. 3 for the cell layouts, the one from DESIGN 1 is not shown because all the radii are 290 μm).

All the geometric parameters of the CMUTs, except the radii, are identical for all three designs. This ensures a meaningful comparison in terms of the influence of the radii distribution on the bandwidth and center frequency of the devices. The thickness of the single-crystal silicon plates is 10 μm, which corresponds to a center frequency of $\sim$400 kHz. The thick-box layers of the devices are 5 μm $\pm$ 5%, the insulation layer thickness is 3 μm (thermally grown silicon dioxide, wet ambient, 19 hours at 1100°C), and the height of the gaps is 2 μm.

Note that all the SOI wafers used for this process (UltraSil Coorporation, Hayward, CA, USA) have been heavily doped for good resistivity (<0.02 ohm-cm, antimony), and the front sides have been carefully polished for direct wafer bonding (<0.3 nm RMS surface roughness).

In order to maintain the center frequency at $\sim$400 kHz, the cell radii range is chosen symmetrically around 290 μm (Fig. 2) for DESIGN 2 [Fig. 3(a)] and 3 [Fig. 3(b)]. However, the radius of the CMUT plate directly changes the static operation point. This is because the larger plates experience a larger static deflection (evacuated cavities), and, thus, will be biased closer to their "individual" pull-in point. Thus, at a certain d.c. bias voltage, the larger plates exhibit a larger average displacement, as shown in Fig. 2 (displacement sensitivity).

In order to avoid that the larger cells are dominating the behavior of the CMUT devices, we intentionally choose a larger number of cells having a radii below 290 μm. Therefore, we use more cells with a radius smaller than 290 μm than cells with a larger radius. For this weighting, depending on the radii of the CMUT plates, we used the displacement sensitivity curve, as depicted in Fig. 2.

Note that for both designs (DESIGN 2 and 3) the larger cells are intentionally positioned more in the outer region of the devices (Fig. 3), and the smaller ones are located more in the center region. In addition, we arranged the different cells as radially symmetric as possible, with the goal of good acoustic beam symmetry.

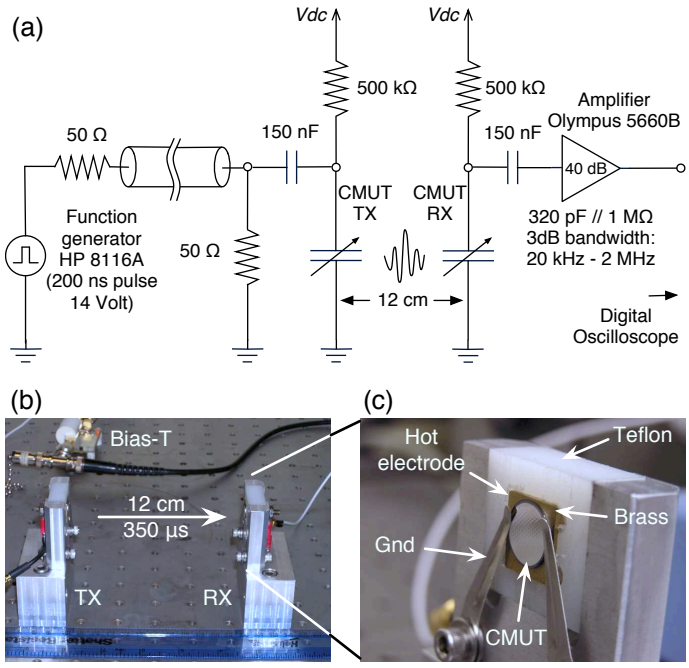

Fig. 4. Schematic of the experimental setup (a) for pitch-catch mode measurements. Photograph of device holders (b) mounted on an air-table for accurate alignment. Detail view of CMUT clamped on device holder (c).

This is in the style of piezoelectric transducers, such as described in [8], or single-element annular transducers (SEATS) [9], having the property of being discs of varying thickness with annular geometry. In these designs the thickness increases from the center (higher frequencies) to the outside (lower frequencies).

III. Experimental Setup

Two CMUTs of each design have been tested in pitch-catch mode (impulse response) with a distance of 12 cm [Fig. 4(a)]. The applied d.c. bias voltage (V_{dc}) was set to 100 V (actual d.c. bias voltage measured at the devices) for both RX and TX side for all measurements.

A function generator HP 8116A (Hewlett-Packard, Palo Alto, CA, USA) was used to excite the transmitting device with a 200-ns pulse with an peak amplitude of 14 V. The receive signals were amplified by 40 dB with a commercially available low-noise ultrasonic amplifier with a bandwidth of 2 MHz (Olympus 5660B, Olympus Industrial, PA, USA). Then the signals were digitized and 64 times averaged by a digital oscilloscope (Infiniium 500 MHz, 2 GS/s, Agilent Technolgies Inc., Palo Alto, CA, USA) and transferred over a GPIB-IEEE488 bus to a common personal computer (PC).

Then a simple Matlab code (Mathworks Inc., Natick, MA, USA) was used to calculate the normalized frequency spectra (FFT, with zero padding and a hanning window), the center frequency, and the -14 db fractional bandwidth.

Note that for this post-processing we used both the entire time signal stored and only the first part of the time signal within the -14 db duration window (ASTM E1065 [10]).

IV. Results and Discussions

The impulse response [Fig. 5(a)] of the pitch-catch configuration equipped with two reference transducers (DESIGN 1) is very narrowband, as expected. The -6 db fractional bandwidth is $\sim$1%. This is typical for a wafer-bonded air-coupled CMUT with evacuated cavities and single-crystal silicon plates. It takes 18 oscillations to reach the peak amplitude of 378 mV, and, thus, a long -14 db duration time of 293 μs can be observed. The beating oscillation origins from a small frequency mismatch between the RX and TX transducers. It can be eliminated by slightly tuning the d.c. bias voltage on either the RX or TX side. For these relatively large CMUTs with thick silicon plates we used SOI wafers with the active layer polished to the target thickness of 10 μm, and not completely epitaxial grown to the target thickness, as for example used in [1]. This explains the difference in resonant frequency, because the 11.85-mm-large devices are coming from different locations on the wafer (4 inch).

The results obtained from DESIGN 2 [Fig. 5(b)] confirm that the signal energy is spread over a wider range of frequencies, on the expense of receive signal amplitude, as expected.

Further, for both cases (DESIGN 2 and 3) the frequency components are located almost symmetrically around the center frequency of 409 kHz (DESIGN 1). This indicates that the displacement sensitivity-weighted distribution of cell radii on the device is beneficial in terms of designing such CMUTs (predictability).

In direct comparison to DESIGN 3 [Fig. 5(c)], one can see that the spreading of the frequency components is too large, resulting in lower values for the fractional bandwidth. This shows that the calculation of the -6 db bandwidth, obtained from the entire time signals (blue curves), i.e. including the long tail of observed beating oscillations, can be very misleading. In fact, such beating oscillations (resonances) also have been observed in the piezoelectric single-element transducers with varying thickness with annular geometry [8].

Due to these beating oscillations, our DESIGN 2 would appear even more narrowband (FBW of 0.63%) than the reference transducer (DESIGN 1). For DESIGN 3 the improvement compared to the reference transducer would be a factor of 2.5.

These pronounced beating oscillations in the tails of the receive signals indicate that several narrowband resonators are operating in unison at certain times. These parts of the signal, however, are not really relevant for many transit-time based ultrasound applications. Examples are range finding, ultrasonic transit-time gas flow meters, anemometry, and various other ultrasound-based sensing applications.

Thus, we added the spectra (red curves in Fig. 5), calculated only from the first part of the time signals (-14 db duration time), as well. For this case, DESIGN 3 outperforms DESIGN 2 with an fractional bandwidth of 18.91%. This is because DESIGN 2 suffers from a single beating oscillation within the -14 db duration time.

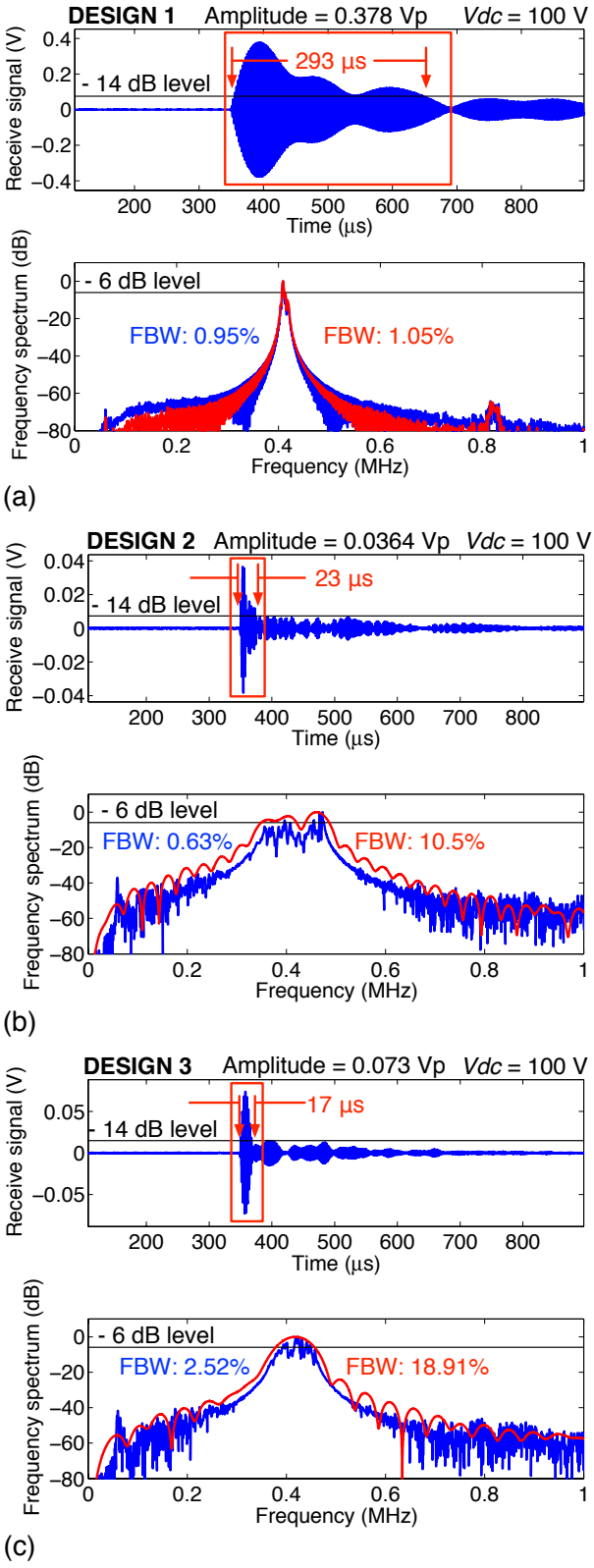

Fig. 5. Time and frequency domain signals, including -14 db duration times (ASTM E1065 [10]) and values for -6 db fractional bandwidths (FBW), for the reference device with all cell radii identical (a), for DESIGN 2 (b) and for DESIGN 3 (c).

V. Conclusion

Our approach of varying the cell radii for wafer-bonded CMUTs with evacuated cavities significantly increases the bandwidth for airborne ultrasound applications. We demonstrated this by fabricating two types of CMUTs and by analyzing time signals and frequency spectra from a pitch-catch configuration (impulse response). A direct comparison to a reference device with constant cell radius shows that the idea of introducing a displacement sensitivity-weighted distribution is beneficial. This ensures an improved predictability of the transducer design concerning the center frequency.

However, in all received time signals from our two new CMUT designs, we observe a beat frequency oscillation after the first couple of oscillations.

Nevertheless, the observed reduction in the -14 db duration time supports the argument that this type of CMUT will be beneficial for many ultrasonic transit-time detection based applications, such as required for gas flow meters.

Acknowledgment

This work was financially supported by AVL List GmbH, Austria and Fluenta Inc., Norway. We thank Dr. Michael Cernusca, Dr. Katarzyna Kudlaty and Dr. Michael Wiesinger, all AVL List GmbH, Graz, Austria, for fruitful discussions. We also thank Larry Randall, Stanford University, for designing and fabricating the device holders (Fig. 4). Further we thank Dr. Steve Vargo, ST Systems USA Inc. for advice on recipes for the deep reactive ion etching steps, and Kim Vu, GE Sensing, Fremont, CA, USA, for performing the DRIE steps.

References

[1] K. K. Park, H. Lee, M. Kupnik, and B. T. Khuri-Yakub, "Fabrication of capacitive micromachined ultrasonic transducers via local oxidation and direct wafer bonding," *Journal of microelectromechanical Systems*, vol. 20, no. 1, pp. 95-103, 2011.

[2] M. N. Senlik, S. Olcum, H. Köymen, and A. Atalar, "Bandwidth, power and noise considerations in airborne CMUTs," *in Proc. IEEE Ultrasonics Symposium*, pp. 438-441, 2009.

[3] C. Bayram, S. Olcum, M. N. Senlik, and A. Atalar, "Bandwidth improvement in a CMUT array with mixed sized elements," *in Proc. IEEE Ultrasonics Symposium*, pp. 1956-1959, 2005.

[4] S. Olcum, M. N. Senlik, and A. Atalar, "Optimization of the gain-bandwidth product of capacitive micromachined ultrasonic transducers," *Ultrasonics, Ferroelectrics and Frequency Control, IEEE Transactions on*, vol. 52, no. 12, pp. 2211–2219, 2005.

[5] M. Kupnik, S. Vaithilingam, K. Torashima, I. O. Wygant, and B. T. Khuri-Yakub, "CMUT fabrication based on a thick buried oxide layer," *in Proc. IEEE Ultrasonics Symposium*, pp. 547-550, 2010.

[6] M. Kupnik and B. T. Khuri-Yakub, "High-temperature electrostatic transducers and fabrication method," *U.S. Patent 7 843 022 B2*, November 30, 2010.

[7] M. Kupnik and B. T. Khuri-Yakub, "Direct wafer bonded 2-D CMUT array," *U.S. Patent 7 846 102 B2*, December 7, 2010.

[8] G. R. Harris and P. M. Gammell "1-3 piezoelectric composite transducers for swept-frequency calibration of hydrophones from 100 kHz to 2 MHz," *J. Acoust. Soc. Am.*, vol. 115, no. 6, pp. 2914–2918, 2004.

[9] J-H. liu, S-Y. Chen, and P-C. Li, "A single-element transducer with nonuniform thickness for high-frequency broadband applications," *Ultrasonics, Ferroelectrics and Frequency Control, IEEE Transactions on*, vol. 56, no. 2, pp. 379–386, 2009.

[10] ASTM E1065-99, "Standard Guide for Evaluating Characteristics of Ultrasonic Search Units," *ASTM International*, 1999.